Raman and surface-enhanced Raman spectroscopic studies of the 15-mer DNA thrombin-binding aptamer

ARTICLE *in* JOURNAL OF RAMAN SPECTROSCOPY · JANUARY 2009

Impact Factor: 2.67 · DOI: 10.1002/Jrs.2428

3 AUTHORS:

Cynthia V Pagba
Georgia Institute of Technology
26 PUBLICATIONS **423** CITATIONS
SEE PROFILE

Stephen M Lane
University of California, Davis
82 PUBLICATIONS **2,375** CITATIONS
SEE PROFILE

Sebastian Wachsmann-Hogiu
University of California, Davis
101 PUBLICATIONS **2,236** CITATIONS
SEE PROFILE

Research Article

Journal of RAMAN SPECTROSCOPY

Received: 6 May 2009 Accepted: 24 June 2009 Published online in Wiley Interscience:

(www.interscience.wiley.com) DOI 10.1002/jrs.2428

Raman and surface-enhanced Raman spectroscopic studies of the 15-mer DNA thrombin-binding aptamer

Cynthia V. Pagba,[a]* Stephen M. Lane[a,b] and Sebastian Wachsmann-Hogiu[a,c]*

Aptamers are single-stranded oligonucleotides that selectively bind to their target molecules owing to their ability to form secondary structures and shapes. The 15-mer (5′-GGTTGGTGTGGTTGG-3′) DNA thrombin-binding aptamer (TBA) binds to thrombin following the formation of a quadruplex structure via the Hoogsten-type G–G interactions. In the present study, Raman and SERS spectra of TBA and thiolated TBA (used to facilitate covalent bonding to metal nanoparticle) in different conditions are investigated. The spectra of the two analogs exhibit vibrations, such as the C8═N7–H2 deformation band at ∼1480 cm^{-1} of the guanine tetrad, that are characteristic of the quadruplex structure in the presence of K^+ ions or at low temperature. Interestingly, SERS spectra of the two analogs differ markedly from their respective normal Raman spectra, possibly due to changes in the conformation of the aptamer upon binding, as well as to the specific interaction of individual vibrational modes with the metal surface. In addition, the SERS spectra of the thiolated aptamer show significant changes with different concentrations, which may be due to different orientation of the molecule with respect to the metal surface. This study provides useful information for the development of label-free aptamer-based SERS sensors and assays.

Supporting information may be found in the online version of this article.

Keywords: Raman spectra; SERS spectra; aptamer; quadruplex; biosensors

Introduction

Aptamers are single-stranded oligonucleotides (DNA or RNA) generated by the process called *systematic evolution of ligands by exponential enrichment* (SELEX).[1,2] Briefly, SELEX involves incubating a target molecule with a random nucleic acid library. The bound molecules are then separated from the unbound molecules (usually by column chromatography). The bound nucleic acids are later detached from the target molecules and amplified by polymerase chain reaction (PCR). This amplified nucleic acid fraction serves as an enriched library for the next cycle. The cycling process is typically done 6–12 times, after which the final enriched library is cloned and sequenced.

Aptamers have been shown to exhibit protein-binding affinities that are comparable to those of corresponding antibodies. Hence, they are being considered as substitutes for bioassays that require molecular recognition. The use of aptamers as biosensors is advantageous because they are less susceptible to denaturation and degradation. They are also smaller than antibodies, which may be significant for applications in which the size is important (e.g. SERS-based assays). They can be synthesized with high purity and reproducibility and are also more easily engineered than the corresponding antibodies. Several aptamers have been developed for certain biological threat agents (e.g. ricin[3] and ricin analog[4] and anthrax spores[5]), cancer biomarkers,[6–9] foodborne pathogens,[10] and other biologically important biomolecules, such as HIV-1 Tat protein,[11,12] cytokines,[13] immunoglobulin E (IgE),[14,15] and thrombin.[16] They are also able to bind to metal ions and small molecules, making them useful in the detection and analysis of environmental pollutants (e.g. polycyclic aromatic hydrocarbons), as well as in drug analysis.[10]

The ability of aptamers to bind to proteins selectively and with high affinity is due to their tendency to form secondary structures and shapes (e.g. quadruplex, hairpin loop, and T-junction)[17,18] in the presence of the target molecule. In particular, the 15-mer (5′-GGTTGGTGTGGTTGG-3′)[16] binds to thrombin following the formation of the quadruplex structure[19] via the Hoogsten-type guanine–guanine interactions (Scheme 1). The formation of this structure was shown and verified by NMR spectroscopy,[19–22] X-ray crystallography,[23] circular dichroism spectroscopy,[24,25] and mass spectrometry.[26] Infrared spectroscopy[27] has also been used to investigate the formation of quadruplex structure by this aptamer by monitoring the characteristic vibrational bands that are associated with such structure. Vibrational spectroscopy is a valuable tool in studying the secondary structures of nucleic

* *Correspondence to: Cynthia V. Pagba and Sebastian Wachsmann-Hogiu, Center for Biophotonics Science and Technology, University of California Davis, Sacramento, CA, USA. E-mail: cvpagba@ucdavis.edu; swachsmann@ucdavis.edu*

a *Center for Biophotonics Science and Technology, University of California Davis, Sacramento, CA, USA*

b *Department of Neurological Surgery, University of California Davis, Sacramento, CA, USA*

c *Department of Pathology and Laboratory Medicine, University of California Davis, Sacramento, CA, USA*

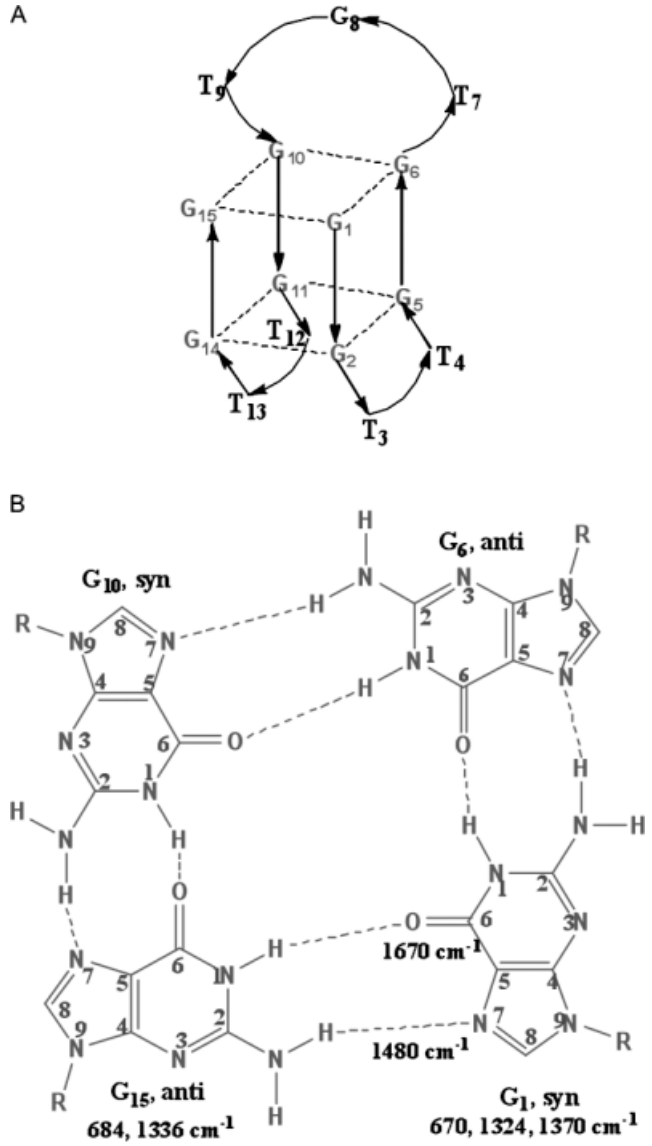

Scheme 1. (A) Quadruplex or chair conformation of the TBA and (B) guanine quartet of the TBA showing the characteristic vibrational frequencies.

acids, as it is sensitive to their different conformations (A, B, or Z) since changes in the conformation often lead to changes in the wavenumbers of the sugar–phosphate backbone and nucleic acid vibrations.[28–33] The infrared spectra of the thrombin-binding aptamer (TBA), as reported by Mondragon-Sanchez *et al.*,[27] clearly showed the vibrational bands corresponding to C2′*endo* sugar conformation (836 cm^{-1}), phosphate backbone vibrations (745, 792, 1095 cm^{-1}) and the presence of intramolecular hydrogen bonding (1480, 1672 cm^{-1}) that are diagnostic of the quadruplex structure.[34–36]

Interestingly, despite the numerous studies on this aptamer,[18,37–39] its Raman and SERS spectroscopic characterization has not yet been reported. Raman spectroscopy is advantageous in biochemical analysis since, unlike IR, it can easily be performed in aqueous systems. In the present study, the Raman and SERS of TBA and thiolated TBA (HS-TBA) in different conditions are investigated. This study will generate information that is valuable in the development of label-free SERS-based bioassays and sensors, currently being undertaken in this laboratory, using this aptamer. The size of the aptamer in the quadruplex form (1.1 nm)[40,41] makes it an ideal capture agent for direct detection SERS-based assays, as the target molecule will still be within the SERS working distance (~10 nm). SERS has been attracting attention in the field of biosensing and assay development owing to its high sensitivity.[42] Presently, available SERS-based assays that require molecular recognition[43–47] make use of Raman active labels as probes, which may not always be advantageous, and, hence, a simpler and direct detection method is desirable.

Materials and Methods

Reagents

Monobasic and dibasic potassium phosphate (KPi) and potassium chloride were obtained from Fisher Scientific. Phosphate buffered saline (PBS) was purchased from USB Corp. Chloroauric acid, ethylene glycol, silver nitrate ($AgNO_3$), sodium citrate, (3-aminopropyl) trimethoxysilane (APTMS) and 6-mercaptohexanol (MH) were purchased from Sigma. The thiolated (5′-HS-$(CH_2)_5$-CH_2-GGTTGGTGTGGTTGG-3′) and unthiolated (5′-GGTTGGTGTGGTTGG-3′) TBAs used were ordered from Sigma Chemical Co. The thiolated sample was supplied as a disulfide form and was used without hydrolysis. DNA samples were studied in water and PBS with 0.1 M KCl. All glassware used were cleaned with aqua regia.

Silver nanoparticle preparation

Silver nanoparticles were prepared following the procedure of Lee and Meisel.[48] Briefly, 20 mg of $AgNO_3$ was dissolved in 100 ml of Milli-Q water and the solution was brought to boiling, after which 20 ml of 0.1% sodium citrate was added dropwise. The mixture was then refluxed for 1 h. The resulting solution was greenish yellow in color. The plasmon resonance was centered at about 412 nm as measured by a Cary UV–vis spectrophotometer.

Glass substrate pretreatment

Glass cover slips were cleaned by sonicating them suceesively in acetone, 1 M NaOH, and Milli-Q water for 15 min each. They were further rinsed with Milli-Q water three times and dried under nitrogen flow. The cover slips were then treated with 5 mM APTMS for 10 min.

Raman measurements

The spontaneous Raman spectra of the thiolated and unthiolated TBAs were recorded using the drop-coating deposition Raman (DCDR) method,[49–51] a technique that takes advantage of the so-called coffee ring effect, that is, the tendency of the dissolved substrate to deposit on the rim of the ring formed upon drying. Briefly, 25 µl of the 10 µM aptamer (in water or PBS-K^+) was deposited on fused silica and allowed to dry at 4 °C or at room temperature. The Raman spectrum was acquired using a homebuilt Raman system with a 60× water objective, 1.32 N.A. and 785 nm excitation wavelength (CrystaLaser). A SpectraPro 2300i Acton spectrometer with a Princeton Instruments Pixis100 CCD was used for dispersing and recording the spectra. An integration time of 180 s and a laser power of 50 mW were used for all spontaneous Raman spectra measurements. The spectra were measured from five different areas (five times each) and the average was obtained.

Journal of RAMAN SPECTROSCOPY

SERS measurements

The stock solution of silver nanoparticles was dialyzed against Milli Q water for 3 h and was diluted with Milli-Q water to get a solution with absorbance of about 0.5. A 10-μl aliquot of this solution was deposited on an APTMS-treated glass cover slip and allowed to air dry at room temperature. The cover slip was then washed with Milli-Q water and blown dry with nitrogen flow. To the immobilized nanoparticles on the film, a 10-μl aliquot of 10 μM stock unthiolated aptamer solution was added and the SERS spectra were recorded immediately. For the thiolated analog, the spectra were measured after a 12-h incubation period at 4 °C and rinsing with PBS-K^+ buffer (pH 7.4).

SERS spectra were acquired using a homebuilt Raman system based on a Till Photonics microscope equipped with a 60×, 1.45 N.A. oil objective, via a SpectraPro 2300i Acton spectrometer with a Princeton Instruments Pixis100 CCD camera, and 647 nm excitation wavelength from an Ar–Kr Innova 70C Coherent laser. An integration time of 60 s and laser power of 100 μW were used for all SERS measurements. The spectra were obtained from five different clusters/aggregates of nanoparticles (five times each) and the average was obtained. The baseline was corrected using a polynomial fit.

Results and Discussion

Spontaneous Raman spectra

Quadruplex (or tetraplex) structures are formed by guanine-rich DNA or RNA residues either by intramolecular folding of a single strand (monomer) or by intermolecular association of two hairpin loops (dimer) or four molecules (tetramer). The formation of this structure is dependent on temperature, DNA concentration, and the presence of certain cations, such as Na^+, K^+, Ca^{2+}, $Pb,^{2+}$ and Sr^{2+} among others. They can be classified as parallel or antiparallel, depending on the orientation of the strands and the conformation of the guanosine residues. In the parallel structure, all guanosines have *anti* conformation, whereas in the antiparallel configuration, guanosine residues alternate between *syn* and *anti* (Scheme 1). TBA, in particular, adopts the latter structure. In aqueous solution, TBA has been found to oscillate between the random coil and the quadruplex form.[52] However, in the presence of certain cations (e.g. K^+, Sr^{2+} and Pb^{2+}) the quadruplex structure predominates.[24,53,54]

Figure 1(A) shows the Raman spectra of TBA in H_2O and PBS-K^+ incubated at room temperature. Although both spectra exhibit characteristic Raman bands associated with the quadruplex structure, their relative intensities are markedly different. For instance, the band around 1480 cm^{-1}, which is assigned to the C8═N7–H2 deformation of the guanine tetrad, is much more intense in the PBS-K^+ spectrum indicating the predominance of the quadruplex form. It should be noted that this band is red-shifted with respect to the N7 vibration of H-bonded guanine in the B-DNA conformation (~1490 cm^{-1})[30,34,55] as well as with the guanine that is not H-bonded (~1496 cm^{-1}).[27,30] This frequency lowering is indicative of strong hydrogen bonding between N7 and H2.

There is also a large difference in the intensities of the guanine breathing mode. This vibrational mode, normally at 650 cm^{-1}, ranges from 600 to 700 cm^{-1} in guanosine depending on the sugar–base conformation. In B-DNA for instance, this mode is shifted to ~682 cm^{-1}, which is diagnostic of C2′-*endo*/*anti* deoxyguanosine (dG) sugar conformation.[29,30,34] The appearance of this band in the spectrum of the aptamer strongly indicates the presence of guanosine in C2′-*endo*/*anti* conformation, which would be expected in an antiparallel quadruplex structure. The band corresponding to C2′-*endo*/*syn* conformation[34] around 671 cm^{-1}, which should also be expected in an antiparallel quadruplex, is obscured by the 685 cm^{-1} band. Its presence, however, is indicated by the 1370 cm^{-1} peak (also attributed to deoxythymidine, dT) and by the 1324 cm^{-1} shoulder to the 1336 cm^{-1} band.[34–36] The intense 1096 cm^{-1} band, which corresponds to the symmetric stretching of the ionized phosphate (PO_2^-) groups in the guanine nucleotides involved in the Hoogsten-base pairing,[27] also supports the presence of the guanine tetrad.

One major difference between the Raman spectra seen in Fig. 1(A) is the 1420–1440 cm^{-1} region. The 1422 cm^{-1} band, assigned to C5′H_2 deformation in C2′ *endo* conformation,[28,29,36] is prominent in aptamer in PBS-K^+, whereas this band appears only as a shoulder to the very intense 1434 cm^{-1} band when the aptamer is in water. This frequency shift can be attributed to the unfolded or random coil structure. This band also is the most intense band in the aptamer in water, indicating that the disordered or random coil structure of the aptamer strand predominates in water.

Another noticeable difference is the C6═O6 stretching mode of guanine. In water, this mode is found around 1663 cm^{-1}, which is characteristic of the free guanine.[27] This band is shifted to a higher wavenumber (~1670 cm^{-1}) for aptamer in PBS-K^+, indicating hydrogen-bond formation. It can also be seen that the intensity of the 1670 cm^{-1} band of TBA in PBS-K^+ is greatly reduced with respect to the 1580 cm^{-1} band, undoubtedly resulting from the strong H-bond formation between O6 and H1.

Figure 1(B) shows the Raman spectrum of TBA in water incubated at room temperature (25 °C) and at 4 °C. The Raman markers (e.g. phosphate backbone at 1096 cm^{-1}, C8═N7–H at 1480 cm^{-1}) of the tetraplex structure are much more intense for the aptamer in water at the lower temperature, which is consistent with previous reports that quadruplex structure formation is favored at low temperatures.[56] The Raman spectrum of TBA incubated at 4 °C closely resembles that of TBA in PBS-K^+ (Fig. 1(A)), strongly indicating the predominance of this structure at this temperature. One noticeable difference is the intensity of the C═O band (~1670 cm^{-1}) relative to the 1580 cm^{-1} band. In PBS-K^+, the intensity of this band is much less compared to that of the 1580 cm^{-1} band, whereas in water at low temperature the intensities of the two bands do not differ much. This is probably due to the added stability of the H-bonding provided by the K^+ ion and/or the interaction of K^+ ion with the H-bonded oxygens of the guanine tetrad.

Interestingly, the Raman spectra (Table 1 and Supporting Information) of the thiolated and unthiolated analogs of the aptamer under similar conditions show only minor differences in the regions between 1000 and 1100 cm^{-1} and 800 and 900 cm^{-1}. The ribose vibration seen at around 850 cm^{-1} in TBA is shifted to 890 cm^{-1} in the HS-TBA analog possibly due to the addition of the hexathiol linker. The bands around 1017 and 1096 cm^{-1} in the spectrum of unthiolated analog are very distinct, whereas in the thiolated analog these bands are convoluted. This broadening of the band is possibly due to the contribution from the symmetric stretching of the C–C backbone (~1070 cm^{-1}) of the hexyl group of the linker. Another interesting observation for both aptamer analogs is the sharpening of the bands at 1180 and 1240 cm^{-1}, attributed to deoxythymidine (dT).

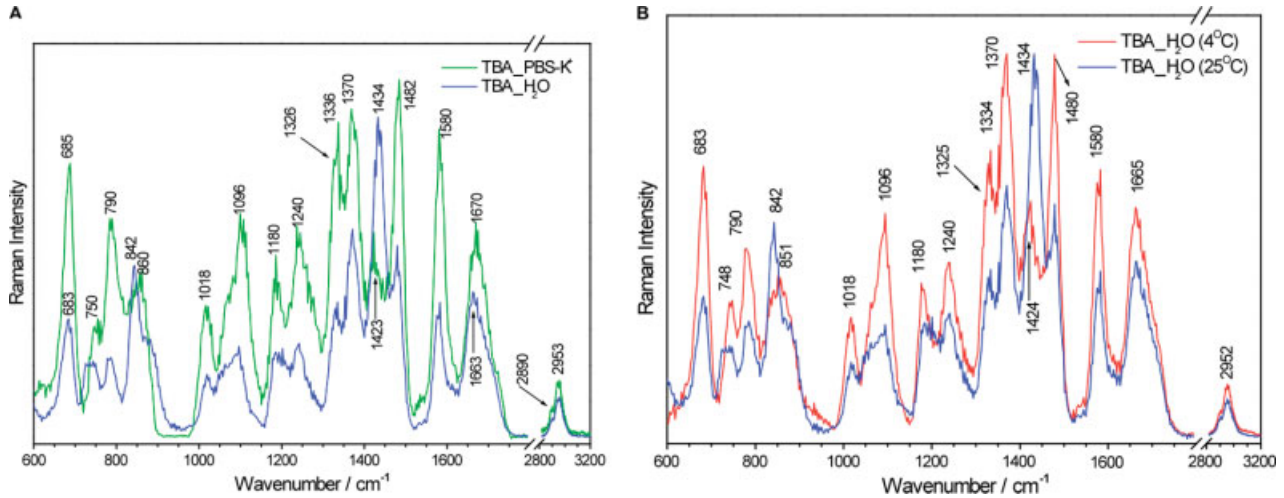

Figure 1. (A) Raman of TBA in PBS with 100 mM KCl (green) and in H_2O (blue) incubated at room temperature (25 °C). (B) Raman of TBA in H_2O incubated at 4 °C (red) and 25 °C (blue). The spectra are normalized with respect to the most intense peak.

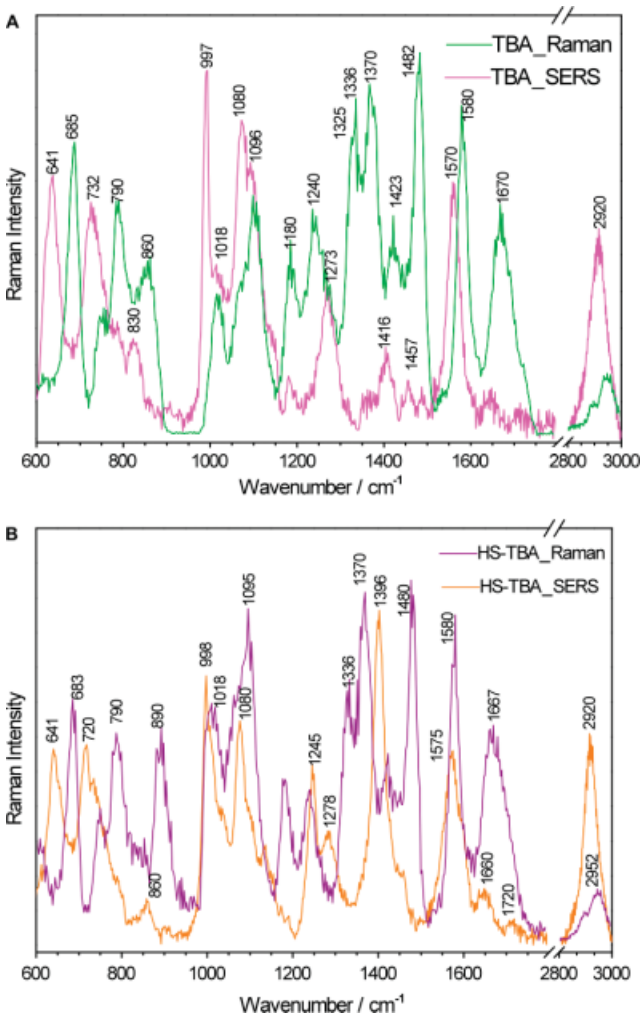

Figure 2. (A) Raman (green) and SERS (magenta) spectra of 10 μM TBA in PBS with 100 mM KCl. (B) Raman (purple) and SERS (orange) spectra of 10 μM HS-TBA in PBS with 100 mM KCl. The spectra are normalized with respect to the most intense peak.

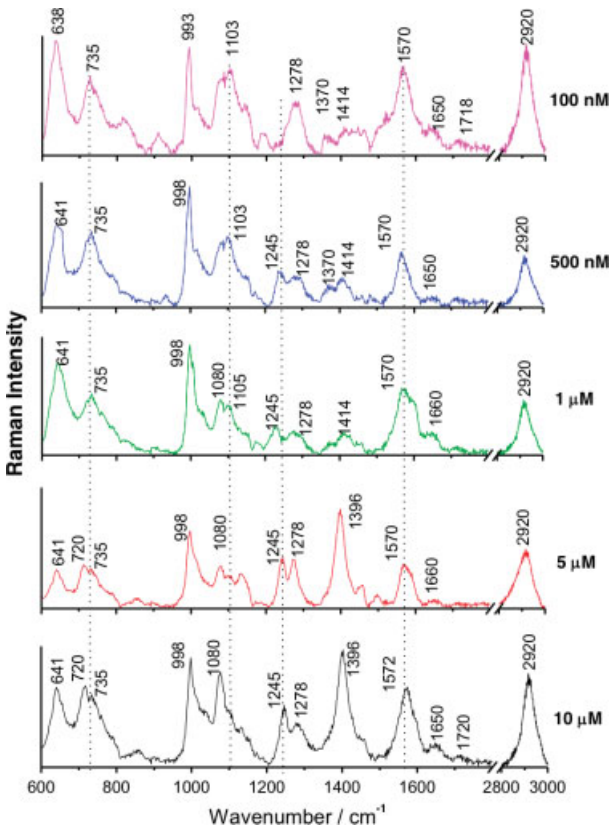

Figure 3. SERS of 100 nm (magenta), 500 nM (blue), 1 μM (green), 5 μM (red), 10 μM (gray) HS-TBA in PBS with 100 mM KCl (green) incubated for 12 hours at 4 C.

Journal of RAMAN SPECTROSCOPY

SERS of TBA and HS-TBA

Figure 2 shows the Raman and SERS spectra of 10 μM solution of unthiolated (A) and thiolated (B) aptamer analogs in PBS-K^+. The aptamer analogs were prepared in PBS-K^+ to ensure that the aptamer is in the quadruplex form before binding to nanoparticles. Interestingly, the SERS spectra of both the thiolated and unthiolated aptamers are drastically different from their corresponding spontaneous Raman spectra. These differences may suggest a change in the structure of the aptamer from a quadruplex geometry to an unfolded state. While this scenario is not impossible, there are other possible explanations that can account for these changes (discussed throughout the text), such as (1) specific interactions of individual vibrational modes with the metal and (2) relative orientation of the molecule with respect to the metal surface. In addition, it is possible that the adsorption of the aptamer to the metal surface leads to enhancement of particular vibrational modes which are normally weak or inactive.

The SERS spectra of the two analogs, though essentially different from each other, share some common features. For instance, the 680 cm^{-1} band, which is diagnostic of the C2′ *endo* conformation of the deoxyguanosine conformation, disappeared and a new band appeared at around 640 cm^{-1}. Nishimura *et al*.[30] assigned the 640 cm^{-1} band to the C2′ *endo/high anti*, wherein the O4–C1–N9–C4 dihedral angle is higher (up to 300°) than the usual *anti* (220°) conformation of guanosine. It is possible that the aptamer molecules are brought closer to each other upon adsorption to the nanoparticle aggregates, and this crowding somehow distorts the ribose–base chain without losing the quadruplex structure since deoxyguanosine is still in C2′ *endo* configuration. The bands around 750 and 790 cm^{-1}, due to antisymmetric and symmetric OPO backbone stretching, respectively, are also missing in the SERS spectra of both analogs. These bands are replaced by bands at 732 cm^{-1} in TBA and by 720 cm^{-1} (with a 735 cm^{-1} shoulder) in HS-TBA. This lowering of wavenumber may be due to the interaction of the phosphodiester backbone with the metal surface and possible partial unfolding of the DNA strand.[57]

Both spectra exhibit sharp peaks around 998 cm^{-1}, which can be attributed to the deoxyribose vibration.[29] The enhanced intensity of this band indicates proximity of this moiety to the surface for both aptamers. A new band around 1275 cm^{-1}, possibly due to the ring stretching and C–H bending of thymine,[58] can be seen in the two SERS spectra. Both spectra also exhibit C–H stretching around 2920 cm^{-1}, which does not coincide with either the symmetric (2890 cm^{-1}) or the antisymmetric deoxyribose C–H stretching (2950 cm^{-1}) found in their respective spontaneous Raman spectra.

Another common feature in the SERS spectra of both aptamers is the absence of the C═O stretching band around 1670 cm^{-1}. The characteristic 1480 cm^{-1} band is also missing in both spectra. These observations may suggest that the aptamer is in its unfolded form, but the absence of the band around 1496 cm^{-1} (which corresponds to the C8═N7 vibration of guanine when it is not hydrogen bonded) indicates otherwise. It is very likely that the guanine tetrads do not interact with the metal since they are not exposed to it. This also explains the absence of the C═O band that is involved in the formation of the tetrad.

One of the major differences between the two SERS spectra is the presence of a strong band around 1396 cm^{-1} in the thiolated aptamer. This can be attributed mostly to the CH_2 deformation, which is shifted from the 1425 cm^{-1} band of the spontaneous Raman spectrum. Kneipp and Fleming[57] reported the appearance of a band at 1391 cm^{-1} in the SERS spectrum of calf thymus DNA instead of the 1422 cm^{-1} band observed in the spontaneous Raman spectrum. It is also likely that there is some contribution from the ring stretching mode of the guanine (1392 cm^{-1}).[30]

Another striking difference in the SERS spectra of the two analogs is the intensity of the ionized phosphate (PO_2^-) backbone vibration (~1100 cm^{-1}). In the unthiolated aptamer, both the 1096 and 1080 cm^{-1} bands are observed, whereas in the thiolated form only the 1080 cm^{-1} band is present. In their IR studies of this aptamer, Mondragon-Sanchez *et al*.[27] assigned the 1077 cm^{-1} band to the stretching mode of phosphate in the loop (Scheme 1(A), $T_7G_8T_9$ loop) of the quadruplex. Although we observed this band only as a shoulder to the 1096 cm^{-1} band in the spontaneous Raman spectrum, we believe that it is due to the same mode. The absence of the 1096 cm^{-1} band and the enhancement of 1080 cm^{-1} band in the SERS spectrum of the thiolated analog suggest that TGT loop is closer to the surface than the guanine tetrad. This scenario is possible if the aptamer is tilted with respect to the surface, and this can only be realized with the thiolated aptamer analog. Since the unthiolated aptamer lacks the functionality required to form a covalent bond with the metal, it is very likely that it is lying flat on the surface. On the other hand, the thiolated analog can adopt a tilted or even standing-up orientation especially at high surface coverage (high aptamer concentration). This can also account for the other observed differences between the SERS spectra of the two analogs.

Concentration dependent SERS spectra of HS-TBA

In order to obtain information on the effect of the orientation of the aptamer with respect to the surface, we varied the concentration of the aptamer and measured SERS spectra. In a recent SERS study of double stranded DNA, Barhoumi *et al*.[59] showed that DNA tends to adopt a tilted or standing-up position at higher surface coverage. The SERS spectra, presented in Fig. 3, clearly exhibit significant changes as the concentration of the aptamer is increased. First, it can be noted that the SERS spectrum of HS-TBA with the lowest concentration (100 nM) resembles that of the unthiolated analog at high concentration (10 μM), which is most likely lying flat on the surface. This observation suggests that at low aptamer concentrations, the molecule lies flat on the surface, which is consistent with previous studies.[59,60]

As the concentration of the aptamer is raised, several changes are observed: namely, (1) the appearance of the 1396 cm^{-1} band, with the loss of the weak band around 1414 cm^{-1}; (2) the growth of the 1080 cm^{-1} band accompanied by the reduction in the intensity of the band around 1103 cm^{-1}; (3) the reduction in the intensity of the 1278 cm^{-1} band with accompanying increase in the intensity of the 1245 cm^{-1} band; and (4) the growth of the 720 cm^{-1} band as the band around 735 cm^{-1} is diminished. These observations clearly demonstrate the effect of orientation of the aptamer on its SERS spectra, which in turn is dependent on the concentration. Although many more studies (both experimental and modeling) are needed to map out the behavior of this aptamer (both thiolated and unthiolated) upon metal adsorption and to precisely assign the vibrational modes, the results of this study provide valuable information that are useful for better design of subsequent experiments.

Conclusion

We have shown that the formation of quadruplex structure at appropriate conditions (presence of K^+ ions or low temperature) can

Table 1. Raman and SERS wavenumbers (in cm^{-1}) of TBA and HS-TBA

Raman wavenumber (cm^{-1})		SERS			
TBA K^+/H_2O, 25 °C/H_2O, 4 °C	HS-TBA K^+/H_2O, 4 °C	TBA	HS-TBA	Assignment	Refs.
		640	640	C2′ *endo/high anti*	[30]
670 (sh)	670 (sh)			dG, C2′ *endo/syn*	[34,36]
685/683/683	684			dG C2′ *endo/anti*	[33,34,46]
			720	OPO str	
		732	735	OPO str	
750/736/748	748			OPO anti-sym	[29]
790/785/	790			OPO sym str	[29,36]
		830 (m)		sugar vib C2′ *endo*	[33,34,36]
865/842/855			860 (m)	sugar vib (C 3′ *endo*)	[33]
	890			sugar vib	
		993	998	deoxyribose vib	[29]
1018	1020	1018		dG, N–H def	[36]
1077(sh)	1077 (sh)	1080	1080	PO_2^- str (TGT loop)	[27]
1096/1095/1094	1095	1103	1103	PO_2^- sym str	[27,33,34]
1180	1180	1180 (m)		dT	[36]
1240	1240		1245	dT, N–H def, C–N str	[36]
		1278	1278	ring str and C–H def of Thymine	[58]
1325 (sh)	1325 (sh)			dG, C2′ *endo/syn*	[34]
1333	1333			dG, C2′ *endo/anti*	[34]
1370	1370	1370	1370 (w)	dT, dG C2′ *endo/syn*	[36]
1423/1434/1424	1423	1416 (w)	1395	Deoxyribosyl ($C5'H_2$) def	[28,29,36]
1482/1480/1479	1480			C8═N7–H2 def	[30,32,34]
		1570	1575	C2═N3 of Guanine	[27]
1580/1582/1583	1580			dG	[27,36]
		1660 (w)	1660 (w)	C6═O6	
1670/1663/1665	1672/1664			C6═O6 of Guanine	[27]
		1720 (vw)	1720 (vw)	C6═O6	
2890 (sh)	2890 (sh)			deoxyribosyl C–H sym str	[29]
		2920	2920	deoxyribosyl C–H str	
2953/2952/2952	2950			deoxyribosyl C–H anti-sym str	[29]

Abbreviations: dG, deoxyguanosine; dT, deoxythymidine; OPO, phophodiester backbone; PO_2^-, ionized phosphate backbone; def, deformation; str, stretching; vib, vibration; sym, symmetri; m, moderate; w, weak; vw, very weak; sh, shoulder.

be conveniently detected using Raman spectroscopy by monitoring the characteristic bands (phosphate backbone, deoxyribose conformation, and ring vibrations) that are associated with such structure. We have also shown that the Raman spectra of the thiolated and unthiolated aptamer are essentially similar. However, their SERS spectra are drastically different. In addition, we observed that the SERS spectra of the thiolated aptamer are dependent on its concentration. We attribute these observed differences in the SERS spectra to the orientation that the aptamer adopts, as well as to partial conformational change upon adsorption to the metal surface. These observations will be relevant in the development of SERS-based label-free assays (currently undertaken in this laboratory) that rely on molecular recognition.

Acknowledgements

This work is supported by funding from the National Science Foundation (NSF) and the Laboratory Directed Research and Development Program of Lawrence Livermore National Laboratory. The Center for Biophotonics Science and Technology is a designated NSF Science and Technology Center, managed by the University of California, Davis, under Cooperative Agreement No. PHY 0120999.

Supporting information

Supporting information may be found in the online version of this article.

References

[1] A. D. Ellington, J. W. Szostak, *Nature* **1990**, *346*, 818.
[2] C. Tuerk, L. Gold, *Science* **1990**, *249*, 505.
[3] J. X. N. S. Y. Y. Jijun Tang, *Electrophoresis* **2006**, *27*, 1303.
[4] J. Tang, T. Yu, L. Guo, J. Xie, N. Shao, Z. He, *Biosens. Bioelectron.* **2007**, *22*, 2456.
[5] J. G. Bruno, J. L. Kiel, *Biosens. Bioelectron.* **1999**, *14*, 457.
[6] B. J. Hicke, C. Marion, Y.-F. Chang, T. Gould, C. K. Lynott, D. Parma, P. G. Schmidt, S. Warren, *J. Biol. Chem.* **2001**, *276*, 48644.
[7] C. Wang, M. Zhang, G. Yang, D. Zhang, H. Ding, H. Wang, M. Fan, B. Shen, N. Shao, *J. Biotechnol.* **2003**, *102*, 15.
[8] J. Ruckman, L. S. Green, J. Beeson, S. Waugh, W. L. Gillette, D. D. Henninger, L. Claesson-Welsh, N. Janjic, *J. Biol. Chem.* **1998**, *273*, 20556.
[9] C.-h. B. Chen, G. A. Chernis, V. Q. Hoang, R. Landgraf, *Proc. Natl. Acad. Sci. U S A* **2003**, *100*, 9226.
[10] S. Tombelli, M. Minunni, M. Mascini, *Biomol. Eng.* **2007**, *24*, 191.

[11] M. Minunni, S. Tombelli, A. Gullotto, E. Luzi, M. Mascini, *Biosens. Bioelectron.* **2004**, *20*, 1149.
[12] S. Tombelli, M. Minunni, E. Luzi, M. Mascini, *Bioelectrochemistry* **2005**, *67*, 135.
[13] J. W. Guthrie, C. L. A. Hamula, H. Zhang, X. C. Le, *Methods* **2006**, *38*, 324.
[14] T. Wiegand, P. Williams, S. Dreskin, M. Jouvin, J. Kinet, D. Tasset, *J. Immunol.* **1996**, *157*, 221.
[15] M. Liss, B. Petersen, H. Wolf, E. Prohaska, *Anal. Chem.* **2002**, *74*, 4488.
[16] L. C. Bock, L. C. Griffin, J. A. Latham, E. H. Vermaas, J. J. Toole, *Nature* **1992**, *355*, 564.
[17] T. Hermann, D. J. Patel, *Science* **2000**, *287*, 820.
[18] N. de-los-Santos-Álvarez, Ma. J. Lobo-Castañón, A. J. Miranda-Ordieres, P. Tuñón-Blanco, *Trends Analyt. Chem. TrAC* **2008**, *27*, 437.
[19] K. Y. Wang, S. H. Krawczyk, N. Bischofberger, S. Swaminathan, P. H. Bolton, *Biochemistry* **1993**, *32*, 11285.
[20] K. Y. Wang, S. McCurdy, R. G. Shea, S. Swaminathan, P. H. Bolton, *Biochemistry* **1993**, *32*, 1899.
[21] R. F. Macaya, P. Schultze, F. W. Smith, J. A. Roe, J. Feigon, *Proc. Natl. Acad. Sci. U S A* **1993**, *90*, 3745.
[22] P. Schultze, R. F. Macaya, J. Feigon, *J. Mol. Biol.* **1994**, *235*, 1532.
[23] K. Padmanabhan, K. P. Padmanabhan, J. D. Ferrara, J. E. Sadler, A. Tulinsky, *J. Biol. Chem.* **1993**, *268*, 17651.
[24] B. I. Kankia, L. A. Marky, *J. Am. Chem. Soc.* **2001**, *123*, 10799.
[25] S. Nagatoishi, Y. Tanaka, K. Tsumoto, *Biochem. Biophys. Res. Commun.* **2007**, *352*, 812.
[26] M. Vairamani, M. L. Gross, *J. Am. Chem. Soc.* **2003**, *125*, 42.
[27] J. A. Mondragon-Sanchez, J. Liquier, R. H. Shafer, E. Taillandier, *J. Biomol. Struct. Dyn.* **2004**, *22*, 365.
[28] J. M. Benevides, G. J. Thomas Jr., *Nucleic Acids Res.* **1983**, *11*, 5747.
[29] W. S. G. J. T. B. Prescott Jr., *Biopolymers* **1984**, *23*, 235.
[30] Y. Nishimura, M. Tsuboi, T. Sato, K. Aoki, *J. Mol. Struct.* **1986**, *146*, 123.
[31] J. M. Benevides, A. H. J. Wang, A. Rich, Y. Kyogoku, G. A. Van der Marel, J. H. Van Boom, G. J. Thomas, *Biochemistry* **1986**, *25*, 41.
[32] J. M. Benevides, A. H. J. Wang, G. A. Van der Marel, J. H. Van Boom, G. J. Thomas, *Biochemistry* **1988**, *27*, 931.
[33] W. L. Peticolas, E. Evertsz, M. J. L. David, E. D. James, *Methods in Enzymology*, Vol. 211, Academic Press: **1992**, p 335.
[34] T. Miura, G. J. Thomas, *Biochemistry* **1994**, *33*, 7848.
[35] T. Miura, G. J. Thomas, *Biochemistry* **1995**, *34*, 9645.
[36] C. Krafft, J. M. Benevides, G. J. Thomas Jr. *Nucleic Acids Res.* **2002**, *30*, 3981.
[37] S. Song, L. Wang, J. Li, C. Fan, J. Zhao, *Trends Analyt. Chem. TrAC* **2008**, *27*, 108.
[38] T. Mairal, V. Cengiz Özalp, P. Lozano Sánchez, M. Mir, I. Katakis, C. O'Sullivan, *Anal. Bioanal. Chem.* **2008**, *390*, 989.
[39] M. Famulok, J. S. Hartig, G. Mayer, *Chem. Rev.* **2007**, *107*, 3715.
[40] P. Alberti, J.-L. Mergny, *Proc. Natl. Acad. Sci. U S A* **2003**, *100*, 1569.
[41] F. He, Y. Tang, S. Wang, Y. Li, D. Zhu, *J. Am. Chem. Soc.* **2005**, *127*, 12343.
[42] K. Hering, D. Cialla, K. Ackermann, T. Dörfer, R. Möller, H. Schneidewind, R. Mattheis, W. Fritzsche, P. Rösch, J. Popp, *Anal. Bioanal. Chem.* **2008**, *390*, 113.
[43] H. Cho, B. R. Baker, S. Wachsmann-Hogiu, C. V. Pagba, T. A. Laurence, S. M. Lane, L. P. Lee, J. B. H. Tok, *Nano Lett.* **2008**, *8*, 4386.
[44] M. D. Porter, R. J. Lipert, L. M. Siperko, G. Wang, R. Narayanana, *Chem. Soc. Rev.* **2008**, *37*, 1001.
[45] R. Narayanan, R. J. Lipert, M. D. Porter, *Anal. Chem.* **2008**, *80*, 2265.
[46] J. D. Driskell, K. M. Kwarta, R. J. Lipert, M. D. Porter, J. D. Neill, J. F. Ridpath, *Anal. Chem.* **2005**, *77*, 6147.
[47] D. S. Grubisha, R. J. Lipert, H.-Y. Park, J. Driskell, M. D. Porter, *Anal. Chem.* **2003**, *75*, 5936.
[48] P. C. Lee, D. Meisel, *J. Phys. Chem.* **1982**, *86*, 3391.
[49] D. Zhang, Y. Xie, M. F. Mrozek, C. Ortiz, V. J. Davisson, D. Ben-Amotz, *Anal. Chem.* **2003**, *75*, 5703.
[50] C. Ortiz, D. Zhang, Y. Xie, A. E. Ribbe, D. Ben-Amotz, *Anal. Biochem.* **2006**, *353*, 157.
[51] A. Barhoumi, D. Zhang, F. Tam, N. J. Halas, *J. Am. Chem. Soc.* **2008**, *130*, 5523.
[52] J. J. Li, X. Fang, W. Tan, *Biochem. Biophys. Res. Commun.* **2002**, *292*, 31.
[53] I. Smirnov, R. H. Shafer, *J. Mol. Biol.* **2000**, *296*, 1.
[54] V. M. Marathias, P. H. Bolton, *Biochemistry* **1999**, *38*, 4355.
[55] J. M. Benevides, M. A. Weiss, G. J. Thomas, *Biochemistry* **1991**, *30*, 5955.
[56] E. Baldrich, A. Restrepo, C. K. O'Sullivan, *Anal. Chem.* **2004**, *76*, 7053.
[57] K. Kneipp, J. Fleming, *J. Mol. Struct.* **1986**, *145*, 173.
[58] T. J. Jvd. T. C. Otto, F. F. M. de Mul, J. Greve, *J. Raman Spectrosc.* **1986**, *17*, 289.
[59] A. Barhoumi, D. Zhang, N. J. Halas, *J. Am. Chem. Soc.* **2008**, *130*, 14040.
[60] C. Boozer, J. Ladd, S. Chen, Q. Yu, J. Homola, S. Jiang, *Anal. Chem.* **2004**, *76*, 6967.